Available online at www.sciencedirect.com
ScienceDirect
Journal of the European Ceramic Society 29 (2009) 1119–1124
www.elsevier.com/locate/jeurceramsoc

Enhanced electrochemical activity and long-term stability of Ni–YSZ anode derived from NiO–YSZ interdispersed composite particles

Kazuyoshi Sato[a,*], Hiroya Abe[a], Teruhiko Misono[b], Kenji Murata[b], Takehisa Fukui[c], Makio Naito[a]

[a] *Joining and Welding Research Institute, Osaka University, 11-1 Mihogaoka, Ibaraki, Osaka 567-0047, Japan*
[b] *Hosokawa Powder Technology Research Institute, 1-9 Shoudai, Tajika, Hirakata, Osaka 573-1132, Japan*
[c] *National Institute of Advanced Industrial Science and Technology, 2266 Anagahora, Shimo-Shidami, Moriyama-ku, Nagoya, Aichi 463-8560, Japan*

Received 15 May 2008; received in revised form 21 July 2008; accepted 30 July 2008
Available online 6 September 2008

Abstract

Nickel oxide–yttira stabilized zirconia (NiO–YSZ) interdispersed composite (IC) particles were prepared by a mechanochemical processing using NiO and YSZ nanoparticles. Transmission electron microscopy (TEM) revealed that primally particles of YSZ (75 nm) and NiO (160 nm) were presented alternatively in the composite particles. Specific surface area (SSA) decreased from 8.6 to 7.1 m^2/g during the mechanochemical processing. The SSA reduction suggested that the chemically bound NiO/YSZ hetero-interfaces were formed during the processing. Scanning electron microscopy with energy dispersive X-ray spectroscopy (SEM-EDS) visualized that the anode made from the IC particles consisted of three-dimensional textured structure of fine Ni and YSZ networks (grain size of them was approximately 500 nm) with 34 vol% of porosity. The anode demonstrated not only low polarization of 152 mV at 1 A/cm^2 even under the operation at 700 °C but also long-term stability for 920 h.

Keywords: Powders-solid state reaction; Nanocomposites; Electrical properties; Ni–YSZ; Fuel cells

1. Introduction

Solid oxide fuel cell (SOFC) is a promising candidate of power generation technology in the 21st century due to its highly efficient power output with clean exhaust. Current efforts were aiming to decrease the cost and to increase the long-term stability of cells and stacks by lowering the operation temperature without reduction of power density. Reduced operation temperature allows replacement of interconnecting material from costly $LaCrO_3$ based ceramics to cost effective stainless steels.[1–5]

Nickel–yttria stabilized zirconia (Ni–YSZ) is the most widely used anode material due to its excellent electrochemical property at high temperature. The electrochemical reaction (hydrogen oxidation) takes place at the triple-phase boundary (TPB) where Ni, YSZ and fuel gas meet.[6,7] The reaction rate strongly depends on the catalytic activity of anode material and the TPB length. Since the former significantly decreases with decreasing the operation temperature, the latter must be increased as much as possible in the limited effective electrode volume to keep high electrochemical performance even at lower temperature. For the TPB enlargement, the anode microstructure such as size and arrangement of Ni and YSZ must be controlled precisely.[7,8]

Prefabrication of the composite particles followed by the electrode fabrication using conventional ceramic processing is a promising way to control the microstructure of composite electrodes.[9–16] Recently, we successfully fabricated coated composite (CC) particles consisted of large core-particle coated by nanoparticles using a mechanochemical processing under dry ambient.[10–12] The composite particles provided well organized electrode microstructure and resulted good electrochemical performance. NiO–YSZ interdispersed composite (IC) particles consisting of NiO and YSZ nanoparticles schematically shown in Fig. 1 are considered to be beneficial for further enlargement of the TPB. However compatibility of high electrochemical performance and long-term stability is still unclear for the Ni–YSZ anode consisted of such fine grains.

The present study concerns the preparation of the NiO–YSZ IC particles using the mechanochemical processing and their

---

[*] Corresponding author. Tel.: +81 668 79 4370; fax: +81 668 79 4370.
E-mail address: k-sato@jwri.osaka-u.ac.jp (K. Sato).

0955-2219/$ – see front matter © 2008 Elsevier Ltd. All rights reserved.
doi:10.1016/j.jeurceramsoc.2008.07.050

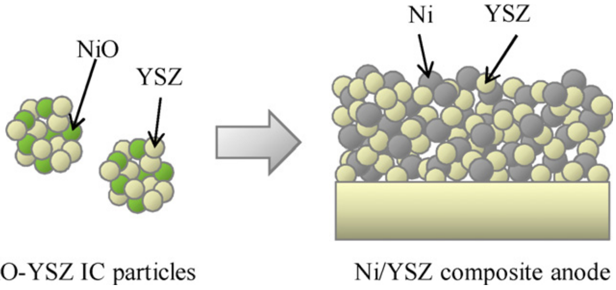

Fig. 1. Schematic illustrations of the NiO–YSZ IC particles and the resultant Ni–YSZ composite anode.

effect on the electrochemical performance improvement and the long-term stability of Ni–YSZ anode.

2. Experimental procedure

2.1. Fabrication of NiO–YSZ IC particles and test cells

The IC particles were prepared by a mechanochemical processing. NiO (Type F, Nikko Rika, Japan) and YSZ (TZ-8Y, Tosoh, Japan) nanoparticles were selected as the starting materials. Before the mechanochemical processing, NiO was mechanically milled alone to make them finer. Specific surface area (SSA) of the NiO and the YSZ nanoparticles measured with a nitrogen gas adsorption based on the Brauner–Emmet–Teller (BET) theory was 5.6 and 13.5 m^2/g, respectively. Corresponding particle diameter of NiO and YSZ was 160 and 75 nm, respectively. The particles were mixed together with the ratio NiO:YSZ = 0.656:0.344 in mass (0.624:0.376 in volume), which corresponded to the ratio Ni:YSZ = 0.5:0.5 in volume at the final anode. The apparatus used to make the IC particles was a high speed attrition type one.[10–13] The apparatus was consisted of the stainless steel chamber and the rotor, and it employed no media ball. The clearance between the rotor and the inside wall of the chamber was fixed at 1 mm. The particles were introduced into the chamber and then the rotor was rotated. When the rotor was rotated, the particles were compressed into the clearance and frequently exposed under the mechanical stressing such as compression and shearing. The operation was conducted under dry ambient without any additives. The rotating speed of the rotor was fixed at 2800 rpm and the total processing time was 40 min.[10]

Electrolyte supported cell was prepared using the following procedures. Firstly, fully dense YSZ electrolyte with the thickness of 300 μm and the diameter of 13 mm was prepared by conventional tape casting followed by sintering at 1450 °C for 2 h. The IC particles mixed with polyethylene glycol (PEG: average molecular weight 400, Aldrich Japan, Japan) were applied on the electrolyte by screen printing and sintered at 1350 °C for 2 h. Then $La_{0.8}Sr_{0.2}MnO_3$ particles mixed with PEG was applied on the opposite side of the electrolyte by screen printing and subsequently sintered at 1100 °C for 2 h. Both electrodes with the area of 0.28 cm^2 were placed symmetrically across the electrolyte.

2.2. Characterization

Structure of the IC particles was characterized by scanning electron microscopy (SEM: ERA-8800FE, Elionix, Japan) and transmission electron microscopy (TEM, JEM-2010, JEOL, Japan) with energy dispersive X-ray spectroscopy (EDS: EDAX, Japan). Anode microstructure was observed by SEM-EDS.

Three electrode-four leads configuration was applied for electrochemical performance testing. All of the testing was conducted at 700 °C. The cell was fixed between alumina tubes with a glass sealant. Pt mesh was placed on both cathode and anode as the current corrector. Pt wire was attached on circumference of the electrolyte as the reference electrode. Pt paste was applied on the reference electrode to improve the electric contact. Firstly, the cell was heated up to 900 °C with the heating rate of 5 °C/min to melt the glass sealant for gas tightening. During the heating, dry air was supplied for the cathode and the reference electrode, and nitrogen was supplied for the anode. Flow rate of all gases was fixed at 0.05 l/min. After the complete gas sealing was confirmed by measuring the inlet and outlet gas flow rates on both the cathode and the anode sides, temperature was decreased to 800 °C with the cooling rate of 5 °C/min. NiO was reduced into Ni by changing the anode gas atmosphere from nitrogen to wet hydrogen containing 3 vol% H_2O at 800 °C. After the open circuit voltage increased to about 1.1 V, the temperature was decreased to 700 °C and the electrochemical performance testing was conducted. Polarization of the anode was measured with DC current interruption technique under the current density up to 1 A/cm^2. Long-term stability of the anode performance was examined under the constant current density at 0.2 A/cm^2 up to 920 h.

3. Results and discussion

Fig. 2(a) shows SEM micrograph of the composite particles. The composite particles consisted of aggregated nanoparticles. Fig. 2(b) shows the detailed structure of a composite particle observed by TEM. NiO and YSZ phases in the composite particle identified by EDS spot analysis were given in the micrograph. The micrograph indicated successful fabrication of the IC particles. NiO and YSZ were presented alternatively, and the size of each particle showed good agreement with that estimated from the SSA of the staring particles (NiO: 160 nm, YSZ: 75 nm). The SSA of the particles decreased from 8.6 and 7.1 m^2/g during the mechanochemical processing. The SSA reduction suggested the formation of chemical bonding at the NiO/YSZ hetero-interfaces.

It is well known that oxide surface is covered by the hydroxyl groups. The hydroxyl groups would play a critical role for formation of the IC particles. Senna et al. reported that the chemically bound hetero-interfaces can be formed during the mechanochemical processing.[17,18] They explained that the bonding was formed according to dehydration–condensation mechanism between the couple of acidic and basic surface hydroxyl groups on the hetero-surfaces. The surface hydroxyl groups of NiO have basic nature since binding energy of Ni–O is lower than O–H.[19] On the other hand, those of YSZ are

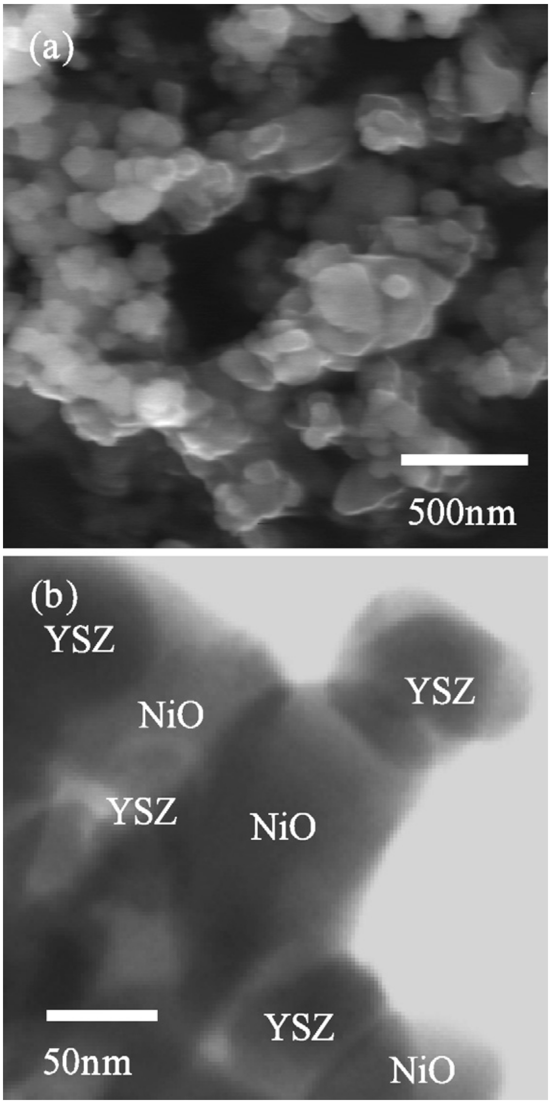

Fig. 2. (a) SEM and (b) TEM micrographs of the NiO–YSZ IC particles.

acidic because of higher binding energy of Zr–O and Y–O compared with O–H.[19] In addition, these interactive surfaces would contribute to form homogeneous mixing state according to well known ordered mixing behavior under the mechanical processing.[20]

Thus, it can be considered for formation mechanism of the IC particles that NiO and YSZ nanoparticles were mixed homogeneously according to ordered mixing behavior due to interactive nature between the acidic and the basic surface hydroxyl groups, forming the chemical bonding at the hetero-interfaces according to the dehydration–condensation mechanism between them. Chemically bound composite particles would have an advantage in the cell fabrication compared with just mixed particles. For example, the composite particles prevent segregation of each component related to the difference in particle size and specific gravity of NiO and YSZ.

Fig. 3 shows SEM micrographs of the anode derived from the IC particles (represented as IC anode in the following text) before the reduction, just after the reduction and after the long-

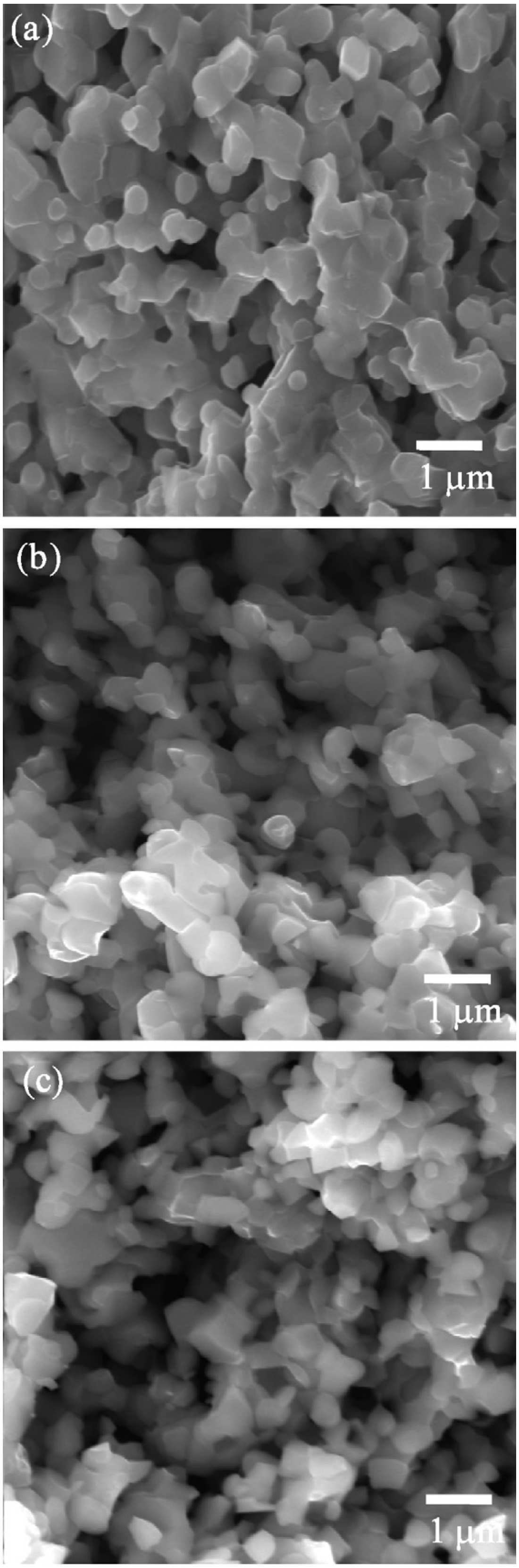

Fig. 3. Cross-sectional SEM image of the IC anode (a) before the reduction; (b) after the reduction; and (c) after the long-term stability testing at 700 °C for 920 h.

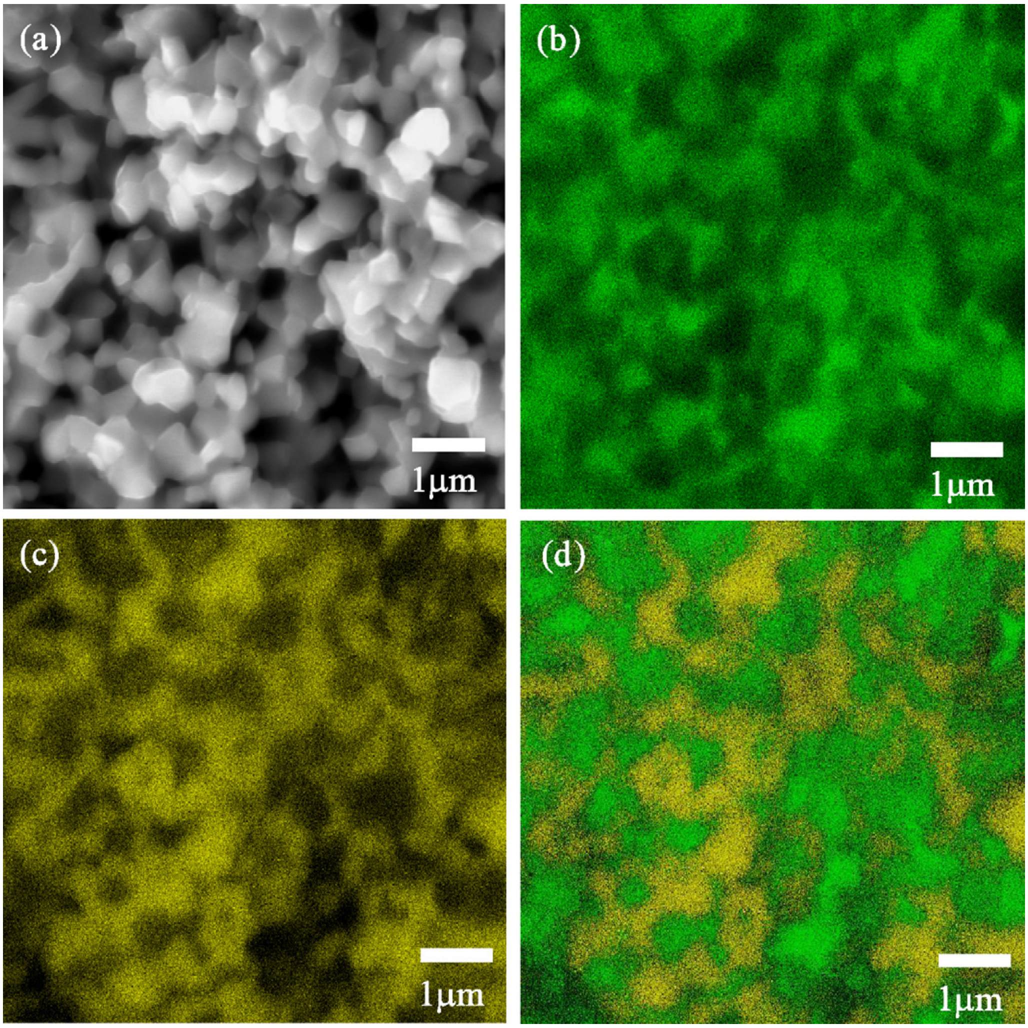

Fig. 4. (a) SEM micrograph and corresponding elemental distribution mappings of (b) Ni; (c) Zr; and (d) Ni(green)/Zr(Yellow) in the IC anode.

term stability testing at 700 °C for 920 h. The IC anode before the reduction consisted of grains smaller than 1 μm without abnormally large grains. NiO shrunk when it was reduced into Ni, and porous structure evolved in the anode. Thus uniform porous structure after the reduction suggested that NiO was uniformly distributed around the uniform three-dimensional network of YSZ framework entire the anode. Even after the long-term stability testing, no significant change was observed in the anode. The grain size was kept to be about 0.5 μm, and no abnormally large grain was observed. The insignificant microstructural change indicated that grain growth of Ni was insignificant in the IC anode under the testing condition.

Fig. 4 shows SEM micrograph and corresponding elemental distribution mappings in the fracture surface of the IC anode after the long-term stability testing at 700 °C for 920 h. Well connected three-dimensional networks of Ni and YSZ were observed in Fig. 4(b) and (c), respectively. Fig. 3(d) showed the combined image of the elemental distributions. The micrograph visualized that the networks of Ni and YSZ grains formed three-dimensional textured structure. The structure clearly reflected homogeneous composite structure of the IC particles shown in Fig. 2(b).

Fig. 5 shows anode polarization curves as the function of current density. Polarization of the anode made from the CC particles consisted of NiO core-particle coated by YSZ nanoparticles (represented as CC anode in the following text)[10] was inserted in the figure. The IC anode showed lower polarization than the CC anode. This implies that the IC anode is better suited for lower temperature operation. Anode polarization is strongly depends on the electrode and gas compositions, and the anode microstructure. The former would be the same, since the compositions of anode material and fuel gas used in this study were the same as in the case of the CC anode.[10] Thus lower polarization of the IC anode compared with the CC anode is ascribed to the formation of longer TPB.

At higher current density region ($\geq$0.3 A/cm^2), slope of the polarization curve in the IC anode was considerably smaller than that of the CC anode. Supplemental experiment indicated that the porosity of the IC anode was about 34% and was similar to that of the CC anode.[11] This result suggested that the difference may not be due to H_2–H_2O counter diffusion effect. Thus, the followings are considerable as the origin of difference at this current density region; (1) adsorption of hydrogen molecules on less reactive surface adjacent to the TPB and/or (2) surface diffusion of the hydrogen atoms from those adjacent surfaces to the reactive TPB.[21] Finer grains of the IC anode provided enlarged adsorption sites due to its larger surface area, and much shorter diffusion path length of adsorbed hydrogen atom to the TPB.

Thus, it can be concluded that fine textured microstructure as shown in Fig. 4 contributed for the TPB enlargement which reduced the anode polarization. Fine grains also enlarged adsorption site of hydrogen molecules and reduced average diffusion path length of hydrogen atoms from adsorption sites to the TPB, both might contribute to reduce the polarization at higher current density region.

Fig. 6 shows long-term stability of the anode performance measured at 700 °C for 920 h. The measurement was conducted under the constant current density at 0.2 A/cm^2. In the early stage of the testing (<30 h), the anode potential only slightly decreased (about 1% from the starting). The potential drop could be ascribed to slight reduction of the effective TPB due to rearrangement or coalescence of Ni grains. Then the voltage kept almost constant from 30 to 920 h. The result evidenced negligible rearrangement and coalescence of Ni grains during this period. The long-term stability of the microstructure was clearly seen in Fig. 3.

Theoretical argument suggested that fine Ni easily rearranges and coalesces during the operation, which is disadvantageous with respect to keep the enlarged TPB over the long-term operation.[22] Recently, Laguna-Bercero and Larrea have fabricated Ni–YSZ cermet by reducing NiO–YSZ directionally solidified eutectic.[23] They found that the formation of crystallographically oriented low energy interfaces between Ni and YSZ significantly retarded rearrangement and coalescence of Ni grains under the operation condition of SOFC. The authors found earlier that the crystallographically oriented interfaces Ni (1 1 1)//YSZ (1 1 1) was formed spontaneously during the operation in the CC anode.[11] These facts suggested that long-term stability of the IC anode was ascribed to the formation of this stable hetero-interface, Ni (1 1 1)//YSZ (1 1 1). Once the stable interface was formed, rearrangement of Ni would be significantly retarded.[23] Thus, the anode potential became constant above 30 h as shown in Fig. 6.

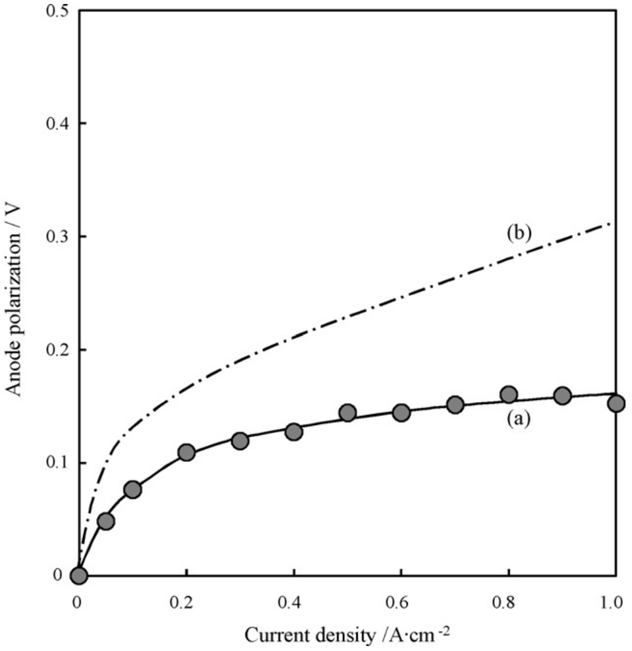

Fig. 5. Anode polarization of the (a) IC and (b) CC[9] anodes at 700 °C.

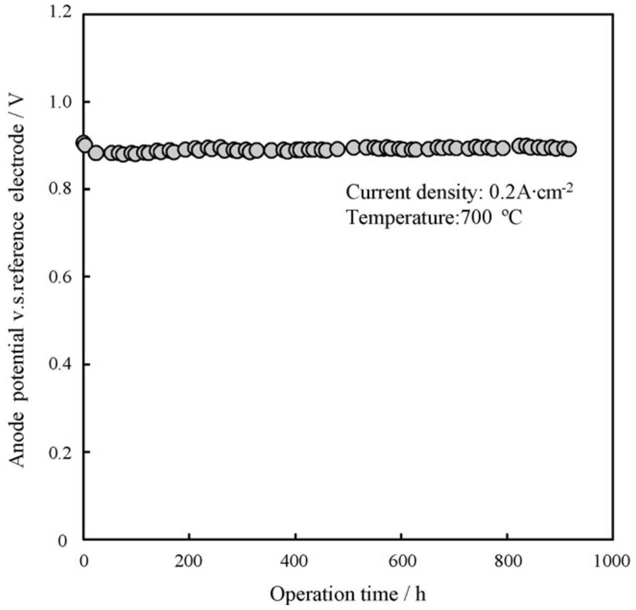

Fig. 6. Long-term stability of the IC anode at 700 °C under the constant current density of 0.2 A/cm^2.

These results indicated that both better electrochemical performance and long-term stability is compatible even using finer Ni grains, if Ni and YSZ networks formed homogeneous textured structure as shown in Fig. 4 due to the formation of enlarged TPB and stable low energy interfaces. Application of further finer Ni and YSZ grains for anode is challenging subject. This will be reported in the future work.

4. Conclusions

The mechanochemically derived NiO–YSZ IC particles from NiO and YSZ nanoparticles provided three-dimensionally textured networks of fine Ni and YSZ grains in the anode. The fine and homogeneous microstructure contributed for TPB enlargement which reduces anode polarization. Fine grains enlarged adsorption sites of hydrogen molecules and reduced average diffusion path length of hydrogen atoms from adsorption site to TPB. These would contribute to reduce the polarization at higher current density region. The IC anode also showed good long-term stability due to suppressed rearrangement and coalescence of Ni during the operation. This can be due to spontaneous formation of stable hetero-interface between Ni and YSZ grains at early stage of the operation.

References

1. Brylewski, T., Nanko, M., Maruyama, T. and Przybylski, K., Application of Fe–16Cr ferritic alloy to interconnector for a solid oxide fuel cell. *Solid State Ionics*, 2001, **143**, 131–150.

2. Horita, T., Xiong, Y. P., Yamaji, K., Sakai, N. and Yokokawa, H., Stability of Fe–Cr alloy interconnects under CH_4–H_2O atmosphere for SOFCs. *J. Power Sources*, 2003, **118**, 35–43.
3. Zeng, Z. and Natesan, K., Corrosion of metallic interconnects for SOFC in fuel gases. *Solid State Ionics*, 2004, **167**, 9–16.
4. Matsuzaki, Y. and Yasuda, I., Electrochemical properties of a SOFC cathode in contact with a chromium-containing alloy separator. *Solid State Ionics*, 2000, **132**, 271–278.
5. Yokokawa, H., Horita, T., Sakai, N., Yamaji, K., Brito, M. E., Xiong, Y.-P. *et al.*, Thermodynamic considerations on Cr poisoning in SOFC cathodes. *Solid State Ionics*, 2006, **177**, 3193–3198.
6. Bieberle, A. and Gauckler, L. J., Reaction mechanism of Ni pattern anodes for solid oxide fuel cells. *Solid State Ionics*, 2000, **135**, 337–345.
7. Brown, M., Primdahl, S. and Mogensen, M., Structure/performance relations for Ni/yttria-stabilized zirconia anodes for solid oxide fuel cells. *J. Electrochem. Soc.*, 2000, **147**, A475–A485.
8. Jiang, S. P., Zhang, S., Zhen, Y. D. and Wang, W., Fabrication and performance of impregnated Ni anodes of solid oxide fuel cells. *J. Am. Ceram. Soc.*, 2005, **88**, 1779–1785.
9. Fukui, T., Ohara, S., Naito, M. and Nogi, K., Performance and stability of SOFC anode fabricated from NiO/YSZ composite particles. *J. Eur. Ceram. Soc.*, 2003, **23**, 2963–2967.
10. Fukui, T., Murata, K., Ohara, S., Abe, H., Naito, M. and Nogi, K., Morphology control of Ni–YSZ cermet anode for lower temperature operation of SOFCs. *J. Power Sources*, 2004, **125**, 17–21.
11. Abe, H., Murata, K., Fukui, T., Moon, W.-J., Kaneko, K. and Naito, M., Microstructural control of Ni–YSZ cermet anode for planer thin-film solid oxide fuel cells. *Thin Solid Films*, 2006, **496**, 49–52.
12. Hagiwara, A., Hobara, N., Takizawa, K., Sato, K., Abe, H. and Naito, M., Preparation and evaluation of mechanochemically fabricated LSM/ScSZ composite materials for SOFC cathodes. *Solid State Ionics*, 2006, **177**, 2967–2977.
13. Misono, T., Murata, K., Fukui, T., Chaichanawong, J., Sato, K., Abe, H. *et al.*, Ni-SDC cermet anode fabricated from NiO–SDC composite powder for intermediate temperature SOFC. *J. Power Sources*, 2006, **157**, 754–757.
14. Kim, S.-D., Moon, H., Hyun, S.-H., Moon, J., Kim, J. and Lee, H.-W., Nanocomposite materials for high-performance and durability of solid oxide fuel cells. *J. Power Sources*, 2006, **163**, 392–397.
15. Wang, F. H., Guo, R. S., Wei, R. T., Zhou, Y., Li, H. L. and Li, S. L., Preparation and properties of Ni/YSZ anode by coating precipitation method. *Mater. Lett.*, 2004, **58**, 3079–3083.
16. Kim, S. D., Moon, H., Hyun, S. H., Moon, J., Kim, J. and Lee, H. W., Performance and durability of Ni-coated YSZ anodes for intermediate temperature solid oxide fuel cells. *Solid State Ionics*, 2006, **177**, 931–938.
17. Watanabe, T., Isobe, T. and Senna, M., Mechanisms of incipient chemical reaction between $Ca(OH)_2$ and SiO_2 under moderate mechanical stressing. I. A solid state acid–base reaction and charge transfer due to complex formation. *J. Solid State Chem.*, 1996, **122**, 74–80.
18. Senna, M., Fujiwara, Y., Isobe, T. and Tanaka, J., Molecular dynamic–molecular orbital combined study on the solid state interfacial reaction under mechanical stressing. *Solid State Ionics*, 2001, **141–142**, 31–38.
19. Weast, R. C., *Handbook of Chemistry and Physics* (*57th ed.*). CRC Press, 1976–1977, pp. F-219–F-225.
20. Hersey, J. H., Ordered mixing: a new concept in powder mixing practice. *Powder Technol.*, 1975, **11**, 41–44.
21. Williford, R. E., Chick, L. A., Maupin, G. D., Simner, S. P. and Stevenson, J. W., Diffusion limitations in the porous anodes of SOFCs. *J. Electrochem. Soc.*, 2003, **150**, A1067–A1072.
22. Mogensen, M. and Skaarup, S., Kinetic and geometric aspects of solid oxide fuel cell electrodes. *Solid State Ionics*, 1996, **86–88**, 1151–1160.
23. Laguna-Bercero, M. A. and Larrea, A., YSZ-induced crystallographic reorientation of Ni particles in Ni–YSZ cermets. *J. Am. Ceram. Soc.*, 2007, **90**, 2954–2960.